THE EUROPEAN
PHYSICAL JOURNAL
SPECIAL TOPICS

Regular Article

Dissociative recombination of N_2H^+: a revisited study

János Zsolt Mezei[1,2,a] , Mehdi A. Ayouz[3], Andrea Orbán[1], Abdillah Abdoulanziz[2], Dahbia Talbi[4], David O. Kashinski[5], Emeric Bron[6], Viatcheslav Kokoouline[7], and Ioan F. Schneider[2,8]

[1] Institute for Nuclear Research (ATOMKI), Bem tér 18/c, Debrecen 4001, Hungary
[2] Laboratoire Ondes et Milieux Complexes, CNRS, Université le Havre Normandie, 53 rue Prony, 76058 Le Havre, France
[3] Laboratoire de Génie des Procédés et Matériaux, CNRS, Université Paris Saclay, CentraleSupelec, 3 rue Joliot-Curie, 91190 Gif-sur-Yvette, France
[4] Laboratoire Univers et Particules de Montpellier, CNRS, Université de Montpellier, Place Eugène Bataillon-CC 72, 34095 Montpellier, France
[5] Photonics Research Center, Bartlett Hall Science Center, Building 753, United States Military Academy, West Point, NY 10996-1790, USA
[6] Laboratoire d'Etudes du Rayonnement et de la Matière en Astrophysique et Atmosphères, Observatoire de Paris, Université PSL, 5, place Jules Janssen, 92195 Meudon, France
[7] Department of Physics, University of Central Florida, 4111 Libra Drive, Orlando, FL 32816, USA
[8] Laboratoire Aimé-Cotton, CNRS, Université Paris-Saclay, Bât. 505, Rue du Belvédère, 91400 Orsay, France

Abstract Dissociative recombination of N_2H^+ is explored in a two-step theoretical study. In a first step, a diatomic (1D) rough model with a frozen NN bond and frozen angles is adopted, in the framework of the multichannel quantum defect theory (MQDT). The importance of the indirect mechanism and of the bending mode is revealed, in spite of the disagreement between our cross section and the experimental one. In the second step, we use our recently elaborated 3D approach based on the normal mode approximation combined with R-matrix theory and MQDT. This approach results in satisfactory agreement with storage-ring measurements, significantly better at very low energy than the former calculations.

1 Introduction

Diazenylium, or N_2H^+, a three-atomic inorganic cation, is one of the first charged species observed in the interstellar medium (ISM), and—in a smaller percentage—in terrestrial environments. It gives astronomers information about the fractional ionization of interstellar molecular clouds and about the chemistry therein, and it is often used as a tracer for molecules that are not as easily detected due to the lack of permanent dipole moment, such as N_2 [1].

N_2H^+ has been detected in a variety of interstellar environments including dark clouds [2], translucent clouds [3], protostellar cores [4], and photodissociation regions [5]. In the ISM N_2H^+ is mainly produced in proton transfer reaction to N_2 from H_3^+ and can be lost via proton transfer to abundant molecules like CO or recombining with slow electrons. N_2H^+ plays also an important role in the nitrogen-rich planetary atmospheres of solar planets and/or moons and exoplanets. For example, in the N_2-dominated ionosphere of Titan, N_2H^+ is formed from the reaction between N_2^+ and H_2,

but is quickly lost via in electron recombination or proton transfer to CH_4 [6]. To predict the abundance of N_2 based on N_2H^+ measurements it is necessary to have insight into the production and destruction mechanisms of N_2H^+.

In the present paper, we plan to study the dissociative recombination (DR) of N_2H^+ in collisions with slow electrons. This process may follow two paths as follows:

$$N_2H^+ + e^- \longrightarrow \left\{ \begin{array}{l} N_2 + H \\ NH + N \end{array} \right. \quad (1)$$
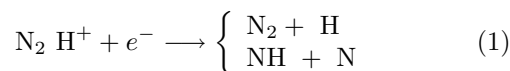
The DR of N_2H^+ has been studied experimentally quite intensively. A Flowing Afterglow Langmuir Probe (FALP) experiment [7] resulted in thermal rate coefficients of the reaction equal to 1.7×10^{-7} cm³s⁻¹ at room temperature. This was somewhat confirmed by later FALP measurements [8, 9], providing a nearly constant rate coefficient of about 2.8×10^{-7} cm³·s⁻¹ over the temperature range from 200 to 500 K. Moreover, by using absorption technics for the final products [10], it was found that the DR of N_2H^+ predominantly goes into the $N_2 + H$ branch of Eq. (1). In contrast to these

[a] e-mail: mezei.zsolt@atomki.hu (corresponding author)

1968

Eur. Phys. J. Spec. Top. (2023) 232:1967–1973

findings, in an experiment performed on CRYRING [11], 64% of the DR was reported in the NH + N branch of Eq. (1). This was disproved eventually by a new flowing afterglow measurement [12] and by a second CRYRING measurement [13] (providing DR cross sections up to 10 eV collision energies), both confirming that more than 90% of the DR goes into the N_2 + H branch.

In addition to these experimental studies, extensive theoretical effort has been provided for the DR of N_2H^+. D. Talbi et al. have published a series of structure calculations [14–17] performed at linear geometries with the NN/NH bond lengths frozen in the framework of the block diagonalisation method [18] combined with GAMESS [19], identifying and characterising both possible—experimentally explored—DR pathways, and showing that N_2 + H should be favoured over N + NH because of the absence of a favourable dissociating state for the N_2 bond breaking [20]. Three repulsive N_2H valence states whose potential energy curves (PECs) cross the ion's one far from the favourable Franck–Condon region were found. This led to the expectation of a small direct DR cross section for vibrationally relaxed ($v^+ = 0$) ions. Meanwhile, a simple model developed by Pratt and Jungen [21] (successfully applied for HCO^+) shows that the DR of polyatomic molecular cations may be quite efficient when the indirect pathway only is relevant.

A more comprehensive alternative method has been elaborated by Douguet et al. [22] and applied to N_2H^+ [23], but also to other polyatomic cations—H_3O^+, H_3^+ [22, 24], HCO^+ and CH_3^+ [24]—providing cross sections and rate coefficients in good agreement with experimental data over a wide energy range. More recently, this method has been used to produce rate coefficients for species of interest for cold plasma applications—BF_2^+ [25]—and for large molecules of astrochemical interest—$CH_2NH_2^+$ [26] and NH_2CHOH^+ [27]. It is based on the computation of the scattering matrix using electron scattering calculations combined with vibronic frame transformation and takes into account all vibrational normal modes of the cations. Fonseca dos Santos et al. [23] have presented results for the indirect dissociative recombination of N_2H^+ using electron scattering calculations with the complex Kohn variational method and they found DR cross sections agreeing well with the CRYRING measurements [13].

In a later study, Fonseca dos Santos et al. [28] have published results on the direct and indirect mechanisms of dissociative recombination of N_2H^+. Electron-scattering calculations responsible for the indirect mechanism were performed using the complex Kohn variational method (scattering matrix, energy positions and autoionization widths of resonant states), while the cross section for the direct dissociation along electronic resonant states is computed with wave-packet calculations using the Multi Configuration Time-Dependent Hartree method [29] with all three internal degrees of freedom considered. The calculated direct DR cross

sections are found smaller by more than an order of magnitude compared to those obtained for the indirect mechanism.

The present paper is structured as follows: In the section following this introduction, we describe the use of our method based on the Multichannel Quantum Defect Theory, in the framework of a 1D diatomic model. This approach is based on the molecular structure data obtained by quantum chemistry calculations of Talbi et al. [14, 16], and demonstrates the importance of the indirect mechanism. In the next section, we revisit the polyatomic (3D) model presented in [23], and perform a new study, within the normal mode approximation, combined with the R-matrix theory and the vibronic frame transformation. We present the obtained DR cross section and compare with the preceding theoretical results and with the storage ring measurements. The paper ends with conclusions and perspectives.

2 Dissociative recombination of N_2H^+: a diatomic 1D model

In the present section, we present our results obtained using the Multichannel Quantum Defect Theory in the frame work of the 1D or *diatomic* model based on molecular data set calculated by Talbi et al. [14, 16].

The efficiency of our stepwise MQDT method in modelling the electron/diatomic cation collisions has been proved in many previous studies on different species, like H_2^+ and its isotopologues [30–35], N_2^+ [36, 37], and many more. The general ideas of our approach were already presented in detail earlier, see for example [38] and, therefore, here we restrict ourselves to the description of the mechanisms.

The reaction (1) involves ionization channels—characterising the scattering of an electron on the target cation—and dissociation channels—relating to atom–atom scattering. The mixing of these channels results in quantum interference of the direct mechanism—in which the capture takes place into a doubly excited dissociative state of the neutral system—with the indirect one—in which the capture occurs via a Rydberg-bound state of the molecule belonging to a closed channel, this state being predissociated by the dissociative one. In both mechanisms the autoionization—based on the existence of open ionization channels—is in competition with the predissociation, and can lead to the excitation or to the de-excitation of the cation.

Depending on the total energy of the system these ionization channels can be open—either as entrance channels, describing the incident electron colliding with the ion in its ground electronic state, or exit channels, describing the autoionization, i.e. resonant elastic scattering, ro-vibrational excitation and de-excitation—or closed—describing the resonant temporary captures into Rydberg states.
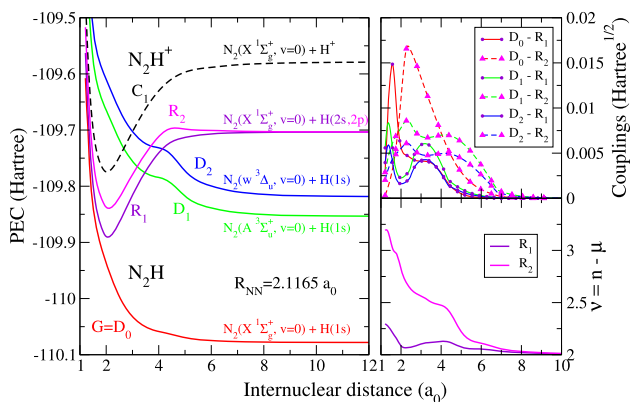
Fig. 1 Molecular data sets used in our 1D-MQDT calculation compiled from [14, 16]. Left panel: Potential energy curves of the molecular cation and neutral system relevant for DR. Upper-right and lower-right panels: The Rydberg-valence electronic couplings and quantum defects

The MQDT treatment of DR requires the a priori knowledge of the PECs of the ion ground state and of the relevant doubly excited, dissociative states of the neutral molecule, as well as for the Rydberg series of mono-excited states represented by the quantum defects. The driving forces of the recombination and excitation processes are the electronic couplings that connects the dissociative and ionization continua.

Figure 1 contains all the molecular data relevant for DR via the "N_2" pathway (a frozen NN bond and frozen angles), the upper branch of Eq. (1) calculated by Talbi et al. [14, 16]. On the left in black, we displayed the PEC of the ground electronic state of N_2H^+ (C_1), and in red, green and blue respectively the PECs of the ground (D_0) and two lowest excited repulsive states of the neutral molecule (D_1, D_2), having dissociative character. The violet (R_1) and magenta (R_2) curves correspond to two representatives (s and p partial waves) of the mono-excited Rydberg series. In the figure we have marked the asymptotic limits for each PEC. In addition to the PECs we present the Rydberg-valence electronic couplings (upper right graph) and the effective principal quantum numbers of the two Rydberg states (lower right graph). They belong to two different Rydberg series, corresponding to different dominant partial waves.

One may notice that, at low collision energies, neither of the three PECs of the dissociative states (D_0, D_1 or D_2) has a favourable crossing with that of the ion. This suggests that the direct DR cross section, at least according to this model, is relatively small.

Indeed, in the first order and assuming that the two dissociative channels D_1 and D_2 are independent, the direct DR cross section via one of these channels reads as [39]:

$$\sigma^{\text{direct}}_{\text{diss}\leftarrow v_i^+} = \frac{\pi\rho}{4\varepsilon} \frac{4(\xi_{v_i^+})^2}{\left[1 + \sum_{v^+}\left(\xi_{v^+}^2\right)^2\right]^2},$$

where $\xi_{v^+} = \pi\langle\chi_{v^+}|V^{\text{el}}(R)|F_{\text{d}}\rangle$. (2)

Here ε stands for the collision energy, v_i^+ is the initial vibrational level of the target cation, ρ gives the multiplicity ratio between neutral molecule and molecular cation states, χ_{v^+} and F_{d} are the vibrational and regular continuum wave functions of the ion ground state and dissociative neutral molecular state (the later calculated in ε), while $V^{\text{el}}(R)$ represents the electronic coupling between the ionization and the dissociation continua. The sum in Eq. (2) is performed on the vibrational levels corresponding to the open ionization channels.

The elements related to the direct cross section are presented in Fig. 2. One can see that the overlap between the vibrational wave function of the ground electronic state of the ion, the continuum wave function of the D_0 dissociative state of the neutral and its electronic coupling with the ionization continuum will lead to a small numerical value, and thus to a very small direct DR cross section.

Nevertheless, the indirect mechanism can be at the origin of the DR process, as it is for example for H_3^+ [40] or HeH^+ [41]. To understand its importance in the case of N_2H^+, we have applied our stepwise MQDT method using the molecular data set presented in Fig. 1. The total cross section, (the reader is referred for details to [38]) is given by:

$$\sigma_{\text{diss}\leftarrow v_i^+} = \frac{\pi}{4\varepsilon} \sum_{l,\Lambda} \rho^\Lambda \sum_j \left|S^\Lambda_{d_j,\,lv_i^+}\right|^2. \quad (3)$$
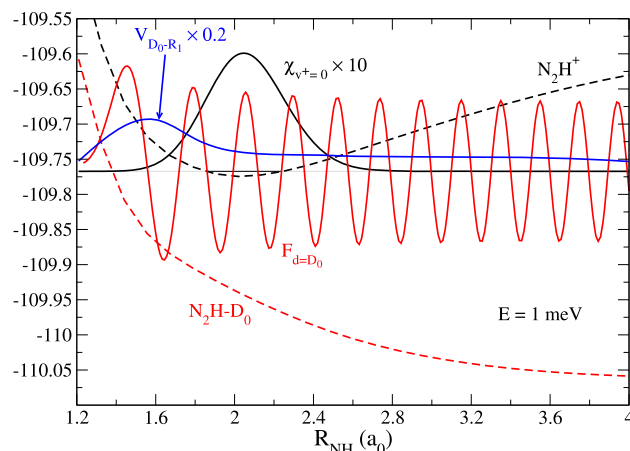
Fig. 2 Main data relevant for the estimation of the direct DR cross section in first order for 1 meV collision energy, according to Eq. (2). The dashed lines stand for the PECs of the ion (black) and for the lowest dissociative state (red) labeled with D_0 in Fig. 1. The black solid line stands for the vibrational wave function of the ion (χ_{v^+} for $v^+ = 0$), the blue solid line represents the Rydberg-valence coupling ($V^{el}(R)$, as in the upper right-hand side graph of Fig. 1), and the red curve stands for the continuum wave function of the dissociative state regular in the origin (F_{d})

1970

Eur. Phys. J. Spec. Top. (2023) 232:1967–1973
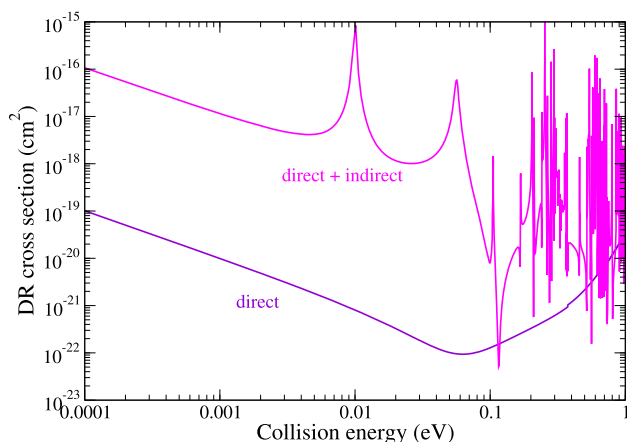
Fig. 3 DR of N_2H^+ at low energy of the incident electron within the 1D MQDT model. Violet: Direct process. Magenta: Total process

Here, l stands for the partial wave of the incoming/outgoing electron and Λ for the projection of the angular momentum on the molecular axis. The sum is performed over all partial waves and symmetries as well as all energetically open dissociative (d_j) states.

Applying our stepwise MQDT method we have calculated the direct and total dissociative recombination (Eq. (3)) cross sections of N_2H^+ in second order by including 31 ionization channels for collision energies up to 1 eV. The rotational effects are neglected. The obtained cross sections for vibrationally relaxed target $(v_i^+ = 0)$ are presented in Fig. 3. The violet and magenta curves stand for the direct and total cross sections. Our results confirm that the direct mechanism is negligible and the indirect process is driving the DR for N_2H^+. The gain obtained by including the Rydberg resonances is more than two orders of magnitude. Although this finding is very important, our total cross section underestimates the CRYRING measurements by more than two orders of magnitude, meaning that the 1D model with a frozen NN bond is not suitable for quantitively describe the DR process. Moreover, besides the stretching mode one has to consider the bending mode of the linear molecule too. In conclusion, an accurate quantitative study needs a 3D description.

3 Dissociative recombination of N_2H^+: the 3D model

The multi-dimensional nature of the vibrational motion of polyatomic ions makes the theoretical study of their dissociative recombination more difficult than that of the diatomic.

We explore the complex dynamics of the DR in this case with a method based on the normal mode approximation combined with the R-matrix theory [42] and

vibronic frame transformation within MQDT. The normal mode approximation is responsible for the vibrational manifold, and usually provides a good description of the vibrational dynamics of molecular systems near the equilibrium geometry. We perform the R-matrix calculations to describe the electron scattering on the target. This provides us the reaction matrix, avoiding the a priori production of the PECS of the electronic states of the neutral and their electronic couplings with the ionization continuum. Eventually, we perform the frame transformation from the body-fixed (or molecular) frame to the laboratory frame.

In our calculation, we follow the general ideas presented in [23], relying on the following assumptions: (1) the rotation of the molecule is neglected, (2) the cross section is averaged over the autoionizing resonances, (3) the autoionization lifetime is assumed to be much longer than the predissociation lifetime and (4) the harmonic approximation is used to describe the vibrational states of the core ion. The electron induced recombination is described in the same way as its excitation but, instead of leaving the vibrationally excited ion, the electron is captured into a Rydberg resonance attached to the vibrational state excited by the electron. If the electron is captured by the ion, the system will most likely dissociate, rather than autoionize. In other words, if the energy of the electron is not sufficient to excite the ion and leave it, the probability of excitation is identical to that of dissociation. Correspondingly, the DR cross section reads as follows:

$$\sigma^{\mathrm{DR}}(\varepsilon) = \frac{\pi}{4\varepsilon} \sum_{i=1}^{n_{\mathrm{modes}}} \theta(\hbar\omega_i - \varepsilon) g_i \sum_{ll'\lambda\lambda'} \left| \frac{\partial S_{l\lambda, l'\lambda'}}{\partial q_i} \right|^2. \tag{4}$$

Here θ is the Heaviside step function, i runs over all the modes of the target molecule, g_i is the degeneracy factor for the mode i, l, λ and l', λ' are the indices of the partial waves and their projections on a chosen quantization axis in the molecular frame of reference. The above formula gives the DR cross section assuming that the target ion is on its ground vibrational level. More details about the theory can be found for example in [25, 38].

The 14 electrons of the linear triatomic N_2H^+ in the equilibrium geometry of the ground electronic $^1\Sigma$ state are distributed in the electronic configuration $(1\sigma)^2(2\sigma)^2(3\sigma)^2(4\sigma)^2(5\sigma)^2(1\pi)^4$. It has three normal modes ($n_{\mathrm{modes}} = 3$): The symmetric (q_4, ω_4) and asymmetric stretching (q_3, ω_3) and the doubly degenerate bending ($q_{1,2}$, $\omega_{1,2}$). Table 1 contains the relevant output of the electron structure calculations we have performed on the target by using the Molpro program suite [45] in the framework of the normal mode approximation. Using cc-pVTZ basis functions at different levels of theory, we have calculated the ground state energy in the optimized equilibrium geometry, the normal mode frequencies and the permanent dipole moments.

Table 1 Equilibrium geometries, normal mode frequencies and permanent dipole moments of the linear N_2H^+ cation calculated with the MOLPRO quantum chemistry suite. Our results are compared with other calculations and with experimental result

Basis	Theory	R_{NN} (Å)	R_{NH} (Å)	$\omega_{1,2}$ (cm^{-1})	ω_3 (cm^{-1})	ω_4 (cm^{-1})	μ_e (debye)
	HF	1.0606	1.0218	823.80	2649.61	3594.16	3.360
	CCSD(T)	1.0992	1.0343	701.86	2280.39	3409.71	0
	MRCI	1.0980	1.0312	714.44	2285.17	3433.82	3.361
	MRCI[a]	1.0998	1.0337	701.78	2273.58	3412.08	3.365
cc-pvtz	CEPA(2)	1.0981	1.0338	688.80	2282.65	3411.65	3.470
	MP2	1.1082	1.0349	704.49	2146.96	3393.49	3.487
	MP4	1.1091	1.0348	680.15	2126.38	3393.11	0
	CISD	1.0835	1.0282	752.03	2443.90	3492.74	–
	CASSCF	1.1005	1.0395	710.58	2274.15	3368.87	3.419
Theory [15, 16]	1D model	1.120	1.074	–	–	–	–
Theory [23]	CAS-CI	–	–	641	2252	3383	3.381
Exp. [43]		–	–	693	2269	3400	–
Exp. [44]		–	–	–	–	–	3.40

[a]CASSCF-MRCI calculation
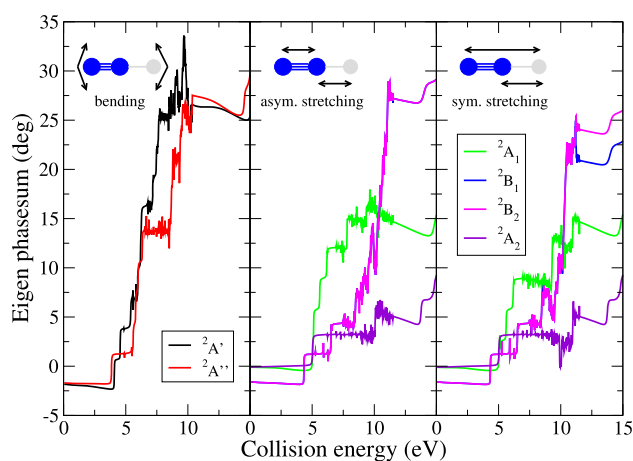
Fig. 4 The sum of eigenphases for the three different normal modes as a function of the electron scattering energy for a displacement of $q_i = 0.05$ along each normal mode

The characterization of the target is followed by electron scattering calculations performed on the "electron+target" system. This part is the bottleneck of our method, since most of the higher level theories and bases functions are not tractable for the scattering calculations performed with UK R-matrix-based Quantemol-N programme suite [46, 47]. The calculations were performed in the abelian subgroup C_s (bending mode) and C_{2v} (stretching modes) and the target ion was assumed to be in its ground electronic state. We have performed Configuration Interaction Self-Consistent Field calculations using Hartree–Fock orbitals by freezing 6 electrons in the core $1(a')^2$, $2(a')^2$, $3(a')^2$ molecular orbitals (MOs) for bending mode, and

$1(a_1)^2$, $2(a_1)^2$, $3(a_1)^2$ for the stretching modes. The remaining 8 electrons are kept free in the active space of the $4a'$, $5a'$, $6a'$, $7a'$, $1a''$, $2a''$ MOs for bending and $4a_1$, $5a_1$, $6a_1$, $1b_1$, $2b_1$, $1b_2$, $2b_2$ MOs for stretching modes, respectively. Virtual molecular orbitals have been added to the Complete Active Space for the augmentation to the continuum orbitals in the following way: 3 virtual MOs of A' and 1 virtual MO of A'' symmetries for the bending mode and 3 A_1, 1 B_1 and 1 B_2 virtual MOs for the stretching ones. A total of nine electronic excited target states are included in our close coupling calculation. We used an R-matrix sphere of radius 14 bohr and in the partial wave expansion we went up to $l = 4$.

At low collision energies, the fixed-nuclei scattering matrix depends only weakly on energy. A quantity convenient for the analysis of the energy dependence of the scattering matrix is the eigenphase sum. Figure 4 displays the eigenphase sum for the three different normal modes corresponding to a small displacement from equilibrium geometry ($q_i = 0.05$) along each normal mode. The variation of the eigenphase sums is smooth for energies below 4.5 eV, suggesting the importance of the indirect mechanism.

The elements of the scattering matrix at a given geometry are computed from the reactance matrix by performing a Cayley transform, and they are expanded to first order in the normal coordinates [25]. To calculate the derivative of the scattering matrix with respect to the normal coordinate, the scattering matrix is evaluated for two coordinate values of each normal mode, namely for $q_i = 0.05$ and 0.5.

Figure 5 shows in black the calculated DR cross sections of N_2H^+ in the framework of the 3D model, by

1972

Eur. Phys. J. Spec. Top. (2023) 232:1967–1973
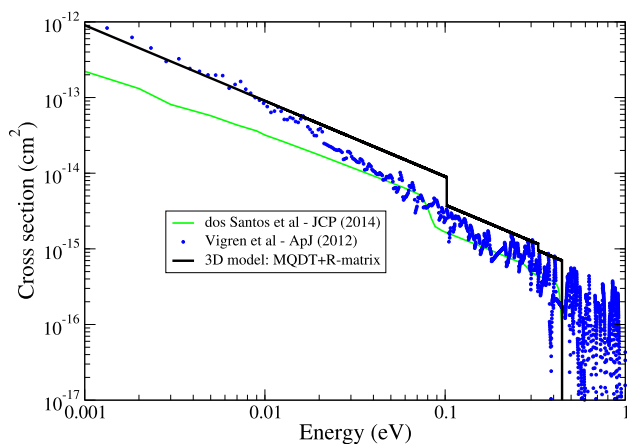
Fig. 5 DR of N_2H^+ at low energy of the incident electron within the 3D model. Blue symbols: CRYRING measurements [13]. Green line: Results obtained with the complex Kohn variational method combined with the normal mode approximation [23]. Black line: Present results relying on R-Matrix-normal mode approximation combined with MQDT frame transformation

applying the formula (4). Our cross section is compared with the CRYRING [13] measured results (blue dots) and with that theoretically produced by Santos et al (green curve) [23].

At very low scattering energies, i.e. below 30 meV, the DR cross section is a smooth function inversely proportional to the incident energy of the electron, as predicted by the Wigner threshold law, whereas at higher energies, it exhibits a drop at each vibrational threshold. Our cross section is in very good agreement with the experimental results at low collision energy, below 30 meV, while at higher collision energies the agreement still remains within a factor of two. Moreover, our calculated cross section shows similar features as those obtained with the complex Kohn-variational method based 3D model [23].

4 Conclusion

In the present work, we have studied the dissociative recombination of the astrochemically relevant diazenylium, N_2H^+ molecular cation.

By using a 1D model with frozen NN bonds we have calculated DR cross sections in the framework of the Multichannel Quantum Defect Theory and pointed out the importance of the indirect mechanism for this process. The obtained total cross section underestimates the storage-ring measurements by more than two orders of magnitude, implying that the 1D model is not sufficient for quantitively describe the DR process. Moreover, besides the stretching modes one has to consider the bending mode of the linear molecule.

Consequently, we have performed a 3D model calculation in the framework of the normal mode approximation combined with R-matrix theory and Multichannel

Quantum Defect Theory. Our results including all three normal modes agree well with the storage-ring measurements and, at very low energy, improve the results of the previous theoretical calculations, relevant for the interstellar media kinetics. The present study reveals the importance of treating the N_2H^+ molecule in its full dimensionality (3D model).

A major issue in the present astrochemical studies is the magnitude of the isotopic effects in the N_2H^+ DR, with respect to both isotopes of N and of H. Calculations on this issue are the subject of an ongoing project.

Availability of data and materials The data underlying this article will be shared on reasonable request to the corresponding author.

Eur. Phys. J. Spec. Top. (2023) 232:1967–1973

1973

References

1. P. Caselli, P.C. Myers, P. Thaddeus, ApJ **455**, L77 (1995)
2. B.E. Turner, ApJ **193**, L83 (1974)
3. B.E. Turner, ApJ **449**, 635 (1995)
4. P. Caselli, C.M. Walmsley, A. Zucconi, M. Tafalla, L. Dore, P.C. Myers, ApJ **565**, 344 (2002)
5. A. Fuente, J. Martin-Pintado, J. Cernicharo, R. Bachiller, A & A **276**, 473 (1993)
6. V. Vuitton, R.V. Yelle, M.J. McEwan, Icarus **191**, 722 (2007)
7. D. Smith, N.G. Adams, ApJ **284**, L13 (1984)
8. V. Poterya, J.L. McLain, N.G. Adams, L.M. Babcock, J. Phys. Chem. A **109**, 7181 (2005)
9. P.A. Lawson, D. Osborne Jr., N.G. Adams, Int. J. Mass Spectrom. **304**, 41 (2011)
10. N.G. Adams, C.R. Herd, M. Gheoghegan, D. Smith, A. Canosa, J.C. Gomet, B.R. Rowe, J.L. Queffelec, M. Morlais, Int. J. Chem. Phys. **94**, 4852 (1991)
11. W.D. Geppert, R. Thomas, J. Semaniak, A. Ehlerding, T.J. Millar, F. Österdahl, M. af Ugglas, N. Djuric, A. Paál, M. Larsson, ApJ **609**, 459 (2004)
12. C.D. Molek, J.L. McLain, V. Poterya, N.G. Adams, J. Phys. Chem. A **111**, 6760 (2007)
13. E. Vigren, V. Zhaunerchyk, M. Hamberg, M. Kaminska, J. Semaniak, M. af Ugglas, M. Larsson, R.D. Thomas, W.D. Geppert, Astrophys. J. **757**, 34 (2012)
14. D. Talbi, Chem. Phys. **332**, 298 (2007)
15. A.P. Hickman, D.O. Kashinski, R.F. Malenda, F. Gatti, D. Talbi, J. Phys. Conf. Ser. **300**, 012016 (2011)
16. D.O. Kashinski, D. Talbi, A.P. Hickman, Chem. Phys. Lett. **529**, 10 (2012)
17. D.O. Kashinski, D. Talbi, A.P. Hickman, EPJ Web Conf. **84**, 03003 (2015)
18. T. Pacher, L.S. Cederbaum, H. Köppel, J. Chem. Phys. **89**, 7367 (1988)
19. M.W. Schmidt et al., J. Comp. Chem. **14**, 1347 (1993)
20. D. Talbi, J. Phys. Conf. Ser. **192**, 012015 (2009)
21. C. Jungen, S.T. Pratt, J. Chem. Phys. **129**, 164311 (2008)
22. N. Douguet, A.E. Orel, I. Mikhailov, I.F. Schneider, C.H. Greene, V. Kokoouline, J. Phys. Conf. Ser. **300**, 012015 (2011)
23. S. Fonseca dos Santos, N. Douguet, V. Kokoouline, A.E. Orel, J. Chem. Phys. **140**, 164308 (2014)
24. N. Douguet, A.E. Orel, C.H. Greene, V. Kokoouline, Phys. Rev. Lett. **108**, 023202 (2012)
25. V. Kokoouline, M. Ayouz, J.Z. Mezei, K. Hassouni, I.F. Schneider, Plasma Sour. Sci. Technol. **27**, 115007 (2018)
26. C.H. Yuen, M.A. Ayouz, N. Balucani, C. Ceccarelli, I.F. Schneider, V. Kokoouline, MNRAS **484**, 659 (2019)
27. M.A. Ayouz, C.H. Yuen, N. Balucani, C. Ceccarelli, I.F. Schneider, V. Kokoouline, MNRAS **490**, 1325 (2019)
28. S. Fonseca dos Santos, V. Ngassam, A.E. Orel, Å. Larson, Phys. Rev. A **94**, 022702 (2016)
29. G.A. Worth, M.H. Beck, A. Jackle, H.-D. Meyer, The MCTDH Package, Version 8.4, University of Heidelberg, Germany (2007). http://mctdh.uni-hd.de
30. O. Motapon, F.O.W. Tamo, X. Urbain, I.F. Schneider, Phys. Rev. A **77**, 052711 (2008)
31. F.O.W. Tamo, H. Buhr, O. Motapon, S. Altevogt, V.M. Adrianarijaona, M. Grieser, L. Lammich, M. Lestinsky, M. Motsch, I. Nevo, S. Novotny, D.A. Orlov, H.B. Pedersen, D. Schwalm, F. Sprenger, X. Urbain, U. Weigel, A. Wolf, I.F. Schneider, Phys. Rev. A **84**, 022710 (2011)
32. K. Chakrabarti, D.R. Backodissa-Kiminou, N. Pop, J.Z. Mezei, O. Motapon, F. Lique, O. Dulieu, A. Wolf, I.F. Schneider, Phys. Rev. A **87**, 022702 (2013)
33. O. Motapon, N. Pop, F. Argoubi, J.Z. Mezei, M.D.E. Epée, A. Faure, M. Telmini, J. Tennyson, I.F. Schneider, Phys. Rev. A **90**, 012706 (2014)
34. M.D.E. Epée, J.Z. Mezei, O. Motapon, N. Pop, I.F. Schneider, MNRAS **455**, 276 (2016)
35. M.D.E. Epée, O. Motapon, N. Pop, I. Felix, E. Roueff, I.F. Schneider, J.Z. Mezei, MNRAS **512**, 424 (2022)
36. D.A. Little, K. Chakrabarti, J.Z. Mezei, I.F. Schneider, J. Tennyson, Phys. Rev. A **90**, 052705 (2014)
37. A. Abdoulanziz, C. Argentin, V. Laporta, K. Chakrabarti, A. Bultel, J. Tennyson, I.F. Schneider, J.Z. Mezei, J. Appl. Phys. **129**, 053303 (2021)
38. J.Z. Mezei, K. Chakrabarti, M.D.E. Epée, O. Motapon, C.H. Yuen, A.A. Mehdi, N. Douguet, S.F. dos Santos, V. Kokoouline, I.F. Schneider, ACS Earth Space Chem. **3**, 2376 (2019)
39. A. Giusti, J. Phys. B Atom Mol. Phys. **13**, 3867 (1980)
40. V. Kokoouline, C.H. Greene, B.D. Esry, Nature **412**, 891 (2001)
41. R. Curík, D. Hvizdos, C.H. Greene, Phys. Rev. Lett. **124**, 043401 (2020)
42. J. Tennyson, Phys. Rep. **491**, 29 (2010)
43. Y. Kaddadj, T.R. Huet, B.D. Rehfuss, C.M. Gabrys, T. Oka, J. Mol. Spectrosc. **163**, 180 (1994)
44. S. Green, J.J.R. Montgomery, P. Thaddeus, Astrophys. J. **193**, L89 (1974)
45. H.-J. Werner, P.J. Knowles, G. Knizia, F.R. Manby, M. Schütz, WIREs Comput. Mol. Sci. **2**, 242 (2012)
46. J. Carr, P. Galiatsatos, J. Gorfinkiel, A. Harvey, M. Lysaght, D. Madden, Z. Maǎín, M. Plummer, J. Tennyson, H.N. Varambhia, Eur. Phys. J. D **66**, 58 (2012)
47. J. Tennyson, D.B. Brown, J.J. Munro, I. Rozum, H.N. Varambhia, N. Vinci, J. Phys. Conf. Ser. **86**, 012001 (2007)